Computational modeling of controlled release of fragrance molecules from industrially relevant capsules

Industry Mentor: Dr. Shyam Vyas, IFF

CHEG/CISC/ECEG/MSEG 867-015
Spring 2023
Prof. Arthi Jayaraman and Prof. Austin Brockmeier

May 11, 2023

Stephen Kronenberger
Ph.D.
Department of Chemical and Biomolecular Engineering
University of Delaware

Destiny King
M.S.
Department of Chemistry
Delaware State University

Tulaja Shrestha
Ph.D.
Department of Chemistry and Biochemistry
University of Delaware

Abstract

The controlled release of active ingredient molecules plays a crucial role in enhancing the performance of fragrance products by prolonging the duration of the scents and preventing active ingredients from releasing too quickly. This project seeks to develop a computational method for studying the controlled release capabilities of active ingredients by calculating their partition and diffusion coefficients, as well as their release profiles, as they diffuse through a polyurea capsule wall. To accomplish this, we used the Martini model, a widely-used coarse-grained force field that groups multiple atoms into a single bead. This approach enables longer simulation run times and larger time steps, which are essential for studying the diffusion, thermodynamic, and dynamic properties of complex systems.

We began by placing the active ingredient molecules codeine and hexanal in a simulation box containing polyurea, water, or other active ingredients. We calculated the diffusion coefficient of each molecule by measuring its mean squared displacement over time. Next, we simulated the active ingredient at different concentrations in a box with either polyurea, water, or other active ingredients (concentrations of these molecules were kept constant to match the density of the material). By using thermodynamic integration, we computed the change in Gibbs free energy of the system as the concentration changed, giving us the partition coefficient, which represents the concentration ratio of a substance between two phases. We then used these diffusion and partition coefficients as inputs into the equation developed by Muro-Suñé and coworkers to generate release profiles.

We compared the release profile plots generated from the simulated data using the diffusion and partition coefficients to those generated using experimental coefficients from Muro-Suñé. However, even after scaling the coefficient values, we observed that the simulated data showed accelerated release compared to the experimental data. Several factors, such as differences in experimental conditions and release media, may have contributed to this result. More investigation and development are necessary, but overall, this project is a promising start toward creating a method for predicting release profiles without relying on experimental data.

1. Introduction:

Fragrances are used in products ranging from cosmetics, shampoos, toiletries, and cleaning items both to enhance the user experience and to make a product distinct and recognizable.[1] Many fragrance molecules (FMs) have high volatility, often requiring additional engineered methods of controlled release to obtain the desired scent and to prolong the lifetime of the FM.[2, 3] Rapid release of the FM is undesirable, motivating studies on controlled release of the FMs for aroma preservation.

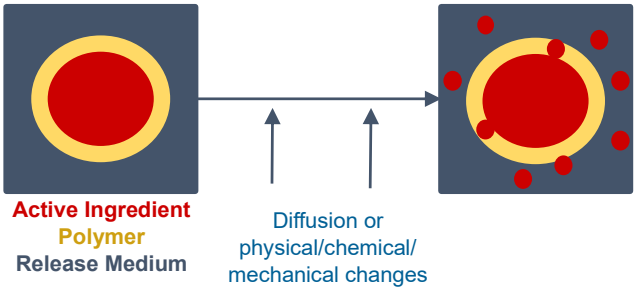

Figure 1: Controlled release of active ingredients through polymeric microcapsule

One way of obtaining the controlled release of fragrances, pesticides, and coatings is through microcapsule encapsulation.[4-6] Various mechanisms, such as diffusive release or physical degradation of the microcapsule, can be used to control the release depending on the desired release profile, as shown in **Figure 1.**[7] This work solely focuses on the prediction of FM release via diffusion.

The broad applications of microcapsule-controlled release have motivated the development of models to predict the release profiles of various fragrance molecules from polymeric microcapsules. The predictive modeling approach helps get the desired release for new and existing chemistries without needing an experimental approach, saving time, energy, and resources. Numerous studies have been done to predict the release profiles of molecules through microcapsules using both computational and mathematical modeling approaches.[8-12] For instance, Muro-Suñé et al. introduce a predictive model that predicted the release profiles, which aligned well with experimental data. Their multiscale approach uses a macroscale model based on Fickian diffusion through a spherical shell (**Eq. 1**), with constitutive relationships informed by experimental data being used to compute the parameters needed for the model. Specifically, they predict the partition coefficients ($K_{m/r}$ and $K_{m/d}$) using the Flory Group Contribution equation of state and the diffusion coefficient (D) from free volume theory.[13, 14] While their predictive model shows good agreement with the experimental data, they require a significant amount of experimental data (including glass transition temperatures, thermal expansivities, and VLE data) to calculate the coefficients used in **Eq.1** (variables are defined in **Appendix Table A1)**.[9]

$$\frac{dC_d}{dt} = \frac{-DA_i}{hV_i} K_{m/d}\, C_{d,init} \exp\left(\frac{-DA_i}{hV_r} K_{m/d}\left(\frac{K_{m/r}}{K_{m/d}} + \frac{V_r}{V_i}\right) t\right) \qquad \text{Eq. 1}$$

Using experimental data to calculate the coefficients used in the predictive macroscale model limits the scope of creating generalizable models for novel chemistries for which experimental data may not exist. Instead, it would be preferred to have a predictive method that does not need experimental data, allowing the method's application to new chemistries without a lengthy collection of experimental data.

Project Goals

Our work aims to address the aforementioned limitation by developing a computational method to predict these coefficients without needing experimental data, thus enabling predictive studies of the release of a given FM through the microcapsule wall. This study has the following objectives:

Objective 1: Build a multiscale model to describe the release profiles of small molecules across a polyurea capsule wall.

Objective 2: Determine the molecular properties needed for constants used in the mathematical model. We calculate those properties using molecular modeling and simulation or other theoretical approaches.

Objective 3: Code the mathematical model in a commonly used numerical modeling platform.

2. Computational Approach

For this project, we leverage the macroscale model developed by Muro-Suñé and coworkers (**Eq. 1**). Of the variables in **Eq. 1**, the most relevant to our work are the diffusion coefficient (D) and the partition coefficients of the FM between the polymer wall and the environment inside the capsule ($K_{m/d}$) and between the polymer wall and the release medium ($K_{m/r}$). We aim to predict the diffusion and partition

coefficients from molecular simulations and use these values to predict the release profile for some FMs.

For simplicity, we assume that the inside of the microcapsule is pure FM, the wall of the microcapsule is polyurea, and the release medium is water in all cases studied. We perform this study for two different FMs: codeine and hexanal. While codeine is not a "fragrance molecule", Muro-Suñé and coworkers used codeine in their work, allowing us to verify our method by comparing our results with theirs. From the list of the FMs suggested by our mentor, we picked hexanal as another FM, given its simple structure that would make it easier for us to run our simulations expediently.

We run coarse-grained (CG) molecular dynamics simulations to determine the required partition and diffusion coefficients for use in the macroscale model defined by **Eq. 1**. We run two types of simulations, which differ in their respective contents of the simulation box and analysis methods to calculate the diffusion and partition coefficients, respectively. Our choice of simulation model, protocols, and analyses are described in further detail in **Sections 2.1-2.3.** After obtaining these coefficients, we solve for the release profile, using methods summarized in **Section 2.4**.

2.1 Coarse-Grained (CG) Model

We use the Martini 3 coarse-grained model to represent the molecules in our simulation.[15] Using CG model helps us improve computational efficiency in simulations and achieve larger length and time scales than using atomistic simulations while maintaining a fairly detailed description of the chemical groups of each molecule. Additionally, using the Martini CG model saves our team the time required to develop a new CG model for all relevant chemistries from scratch; this pre-built CG model is valuable for the semester-long timeframe of this project.

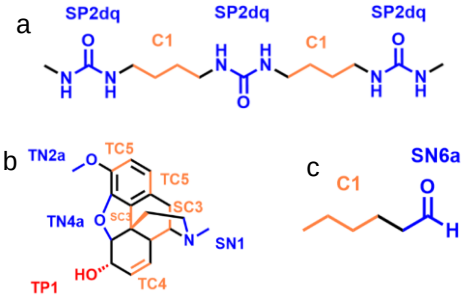

Figure 2. MARTINI 3 bead models of polyurea (a) codeine (b) and hexanal (c) used in our simulations. The description of the relevant MARTINI mapping letters (SP2dq, TC5 etc.) is described briefly in **Appendix Table A5** and detailed information can be found in Ref. 14.

CG beads: In general, in the Martini CG model, one CG bead represents groups of 2-4 atoms and is parameterized to account for the size, polarity, and hydrogen bonding tendencies between different atoms.[15] **Appendix Table A5** lists the types of beads and the chemical features they represent. We assigned Martini bead types to the atoms in water, polyurea, hexanal, and codeine using the example mappings in the Martini 3 paper and our chemical intuition as depicted in **Figure 2**. Overall, our approach to bead assignment in Martini 3 yields more precise molecular models that closely resemble their real-world counterparts.

Bonded Potentials: Bonds and angles are defined using harmonic potentials. Generally, one optimizes the bonded potential parameters in a Martini model by mapping from atomistic simulations. Due to time restrictions for this project, we relied on previously developed models (e.g., polyurea, water) or obtained the equilibrium bond lengths and angles by performing an energy minimization on the chemical structure of the FM in the Avogadro software.[16] To ensure that we have accurate bond lengths and angles, we cross-referenced the values with common literature values. All harmonic bond and angle force constants were set to 1250 kJ/(mol.Å^2) and 50 kJ/(mol.rad^2), as commonly used in the Martini force field. For polyurea, the bond and angle parameters were adapted from a similar CG model of polyurea in the literature.[17] Lastly, the Martini model represents four water molecules as a single water bead.[15, 18]

Non-bonded potentials: The Martini force field uses the 12-6 Lennard Jones potential to model all nonbonded interactions between CG beads, with the various ε and σ tabulated for each combination of bead types.[15] We found the parameter ε prescribed by the Martini 3 model describing the interaction strength between water beads to be too small, resulting in gaseous behavior, so while the Martini 3 nonbonded parameters were used for all water-other bead type potentials, the water-water parameters were adapted from Martini 2, which models the water beads with ε = 5.0kJ/mol and σ = 0.47nm.[18]

2.2 Simulation Protocol: Partition Coefficient Simulations

The partition coefficient is defined as the ratio between the concentrations of a substance in two media or phases at equilibrium. To calculate partition coefficients, we compute the free energy change of a single FM as it is removed from each environment (pure FM, polyurea, and water) using thermodynamic integration (TI). TI is a method of computing free energy changes from molecular simulation, where the thermodynamic path between two states is defined in terms of a coupling parameter, λ, which ranges

from 0 to 1. The change in free energy is computed by integration over the partial derivatives of potential energy with respect to λ (**Eq. 2**). The variables included in this equation are described in **Appendix Table A2**, and further description of our specific implementation of TI to compute partition coefficients is in **Appendix Section A4**.

$$\Delta G = \int_0^1 \langle \frac{\partial U}{\partial \lambda} \rangle_\lambda \, d\lambda \approx \int_0^1 \frac{\langle U(\lambda + d\lambda) - U(\lambda) \rangle_\lambda}{d\lambda} d\lambda \qquad \text{Eq. 2}$$

All simulations are run in the NPT ensemble at 300 K and 1 bar, with 3 fs timesteps. A Nosé-Hoover thermostat and barostat are used with respective damping coefficients of 10 and 1000 timesteps. Simulations in the water, pure FM, and polyurea environments are run with the number of water beads, FM, and polyurea chains chosen to match the bulk density of these materials in a box with side lengths of 50 Å (100 Å for polyurea). A snapshot of the simulation setup is included in **Appendix Figure A5 (b-d)**. We performed three trials of each simulation to confirm consistency in the computation of the partition coefficients. Simulations were implemented using the Large-scale Atomic/Molecular Massively Parallel Simulator (LAMMPS) software.[19]

We note that there have been many developments in free energy calculations from simulations that could provide potential improvements or validations over the finite difference TI we have used here. Some possible options to improve or further validate our approach are detailed in **Section 4.**

2.3 Simulation Protocol: Diffusion Coefficient Simulations

Diffusion coefficient is the amount of a particular substance that diffuses across a unit area in 1 s under the influence of a concentration gradient of one unit. To calculate the diffusion coefficient, we simulate 5 FMs in a system of polyurea chains to compute the diffusion coefficient of the FM through the polymer microcapsule wall. 442 polyurea chains composed of 10 repeats each (see the Martini model in **Fig. 2**), corresponding to a volume fraction of 0.4, are simulated in melt-like conditions in a box with side length 100 Å. The simulations were performed in the NVT ensemble at a temperature of 300 K with a timestep of 3 fs. A Nosé-Hoover thermostat with a damping coefficient of 10 timesteps is used. A snapshot of the simulation is shown in **Appendix Figure A5 (a)**.Three independent trials of each simulation were performed to confirm the consistency of the computation of the diffusion coefficient. Simulations were implemented using the LAMMPS software.[19]

The polyurea comprising the microcapsule wall is glassy, making the direct measurement of the diffusion coefficient from simulation unfeasible due to the long relaxation times for glassy polymeric systems. This was confirmed in our preliminary testing of the diffusion simulations using the full Martini polyurea interactions at the density of bulk polyurea (**Appendix Fig. A1**). These results showed poor statistics of the MSD data resulting from the glassy system, where neither the FM nor the polyurea chains move a significant distance over the course of the simulation.

For this reason, *in the diffusion simulations*, we treat the system as meltlike, with polyurea-polyurea interactions modeled using the purely repulsive Weeks-Chandler-Andersen potential, while maintaining the 12-6 LJ potential for all polyurea-FM interactions. We also use a lower volume fraction of polyurea chains (Φ = 0.4), than that which would replicate the real bulk density of polyurea. With this simplification, we aim to focus on the relative interactions between the FM and the polyurea, while obtaining data with reliable statistics to use in the macroscale release model. Further discussion of the corrections we implemented to account for these described deviations from reality is described in **Section 3**, while some possible alternatives to our approach as described in **Section 4**.

We compute D using the Einstein relation (**Eq. 3**): where N is the number of diffusing molecules, and r_i is the center of mass of the diffusing molecule.

$$D = \frac{1}{6} \lim_{t \to \infty} \frac{d}{dt} \langle \frac{1}{N} \sum_{i=1}^{N} |r_i(t) - r_i(0)|^2 \rangle \qquad \text{Eq. 3}$$

To compute D via **Eq. 3**, we compute the center of mass of each FM every 100,000 timesteps. Each time point for the MSD calculation consists of averages of the molecules' center of mass over the entire simulation period with a time lag Δt = 100,000 timesteps. The MSD curves for each of the 5 FMs are averaged together, yielding the final MSD data used in **Eq. 3** to compute D. D is computed only over the timescale of the simulation where the plot of the MSD vs. time is linear (also known as the "middle" region).[20] The middle region was confirmed by plotting the MSD vs. time on a log-log plot and identifying the region where the slope is near 1, as shown in **Appendix Figure A2**.

2.4 Analytical Solution of Macroscale Release Model

Lastly, we use the diffusion and partition coefficients obtained from our simulations in the macroscale diffusion model to obtain the release profile. The ordinary differential equation (ODE) in **Eq. 1** describes

the release of the fragrance molecule through a microcapsule of a given size. Muro-Suñé et al., solved this differential equation for a discretized normal distribution of capsule sizes and computed the combined release across all capsule sizes.[9] Similarly, we analytically solve the ODE and calculate the concentration from the resulting analytical expression (all variables for **Eq. 4** are described in **Appendix Table A4**) for each capsule size. Then, like Muro-Suñé et al., we compute the combined release across all capsule sizes. Lastly, to quantify the error in our release profiles from the error in the diffusion and partition coefficients obtained from simulation, we repeat this solution process for 1,000 bootstrapped samples of D, $K_{m/d}$, and $K_{m/r}$, with each sample being drawn from a normal distribution with the mean and standard deviation being equivalent to those obtained from the simulation trials.

$$C_d(t) = \frac{V_r\, C_{d,init}}{V_i\left(\frac{K_{m/r}}{K_{m/d}} + \frac{V_r}{V_i}\right)}\left[\exp\left(\frac{-DA_i}{hV_r} K_{m/d}\left(\frac{K_{m/r}}{K_{m/d}} + \frac{V_r}{V_i}\right)t\right) - 1\right] + C_{d,init} \qquad \text{Eq. 4}$$

3. Results and Discussion

In **Table 1**, we report the computed free energy changes of codeine and hexanal in each required environment (water, pure FM, and polyurea). The individual plots of dU/dλ used to compute these free energy changes are included in **Appendix Figure A3.**

	$\Delta G_{env.\rightarrow 0}$ (kJ/mol)			Partition Coefficients	
Environment	**Other FM**	**Polyurea**	**Water**	**$\log(K_{m/d})$**	**$\log(K_{m/r})$**
Codeine	60.88 (3.22)	85.32 (4.06)	11.18 (1.09)	4.25 (0.90)	12.9 (0.73)
Hexanal	24.81 (0.77)	38.62 (2.12)	5.87 (0.53)	2.40 (0.39)	5.70 (0.38)

Table 1: Results from the partition coefficient simulations described in **Section 2.2**. Values in parentheses indicate the standard deviation of three trials.

For all computed free energy changes, the standard deviation across three trials is less than 10% of the mean value, indicating that the method is consistent. The computed free energy changes indicate that both FMs will have the highest proclivity for polyurea, then more FMs of the same type, then water, with a higher free energy change for an environment indicating a preference for the FM to be in that environment.

These results qualitatively agree with expectations based on our Martini model (**Fig. 2**). For one, our polyurea model includes hydrogen-bonding donor beads, while both FMs have hydrogen bonding acceptors, explaining the preference for both FMs to be in polyurea. Second, codeine has a greater number of hydrogen bond acceptors than hexanal, suggesting that its computed free energy change in polyurea is higher than that of hexanal. The preference of both FMs to be surrounded by other FMs of the same type rather than surrounded by water also agrees with our knowledge that both FMs are water insoluble.

In **Table 2**, we show the results of the diffusion simulations for both codeine and hexanal. From **Table 2**, we see that the hexanal diffuses faster than codeine in polyurea, which was expected since it is a significantly smaller molecule than codeine. As expected, due to neglecting the polymer-polymer interactions and reducing the density of the polyurea in our diffusion simulations, the diffusion coefficients we obtain are orders of magnitude larger than the values approximated by Muro-Suñé et al., who obtained a diffusion coefficient of 1.027e-19 m^2/s for codeine in polyurea.

	Diffusion Coefficient (10^{-9} m^2/s)
Codeine	1.954 (0.082)
Hexanal	7.162 (1.862)

Table 2: Results for the diffusion simulations described in **Section 2.3**. Values in parentheses indicate the standard deviation over three trials.

Finally, based on the values obtained from our simulation, we can calculate the release profiles over time, as described in **Section 2.4**. Here, we keep all other parameters describing the microcapsule size distribution, thickness, and release volume the same as was used by Muro-Suñé et al. These parameters are summarized in **Appendix Table A6,** and the computed release profiles are shown in **Figure 4.**

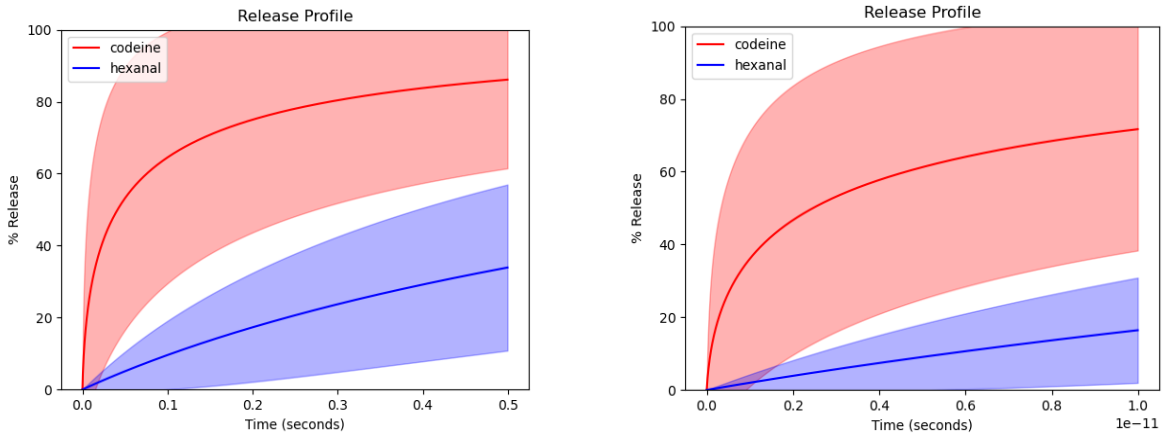

Figure 4. Release profiles for codeine and hexanal computed from the macroscale diffusion model (Eqs. 1 and 4) using diffusion and partition coefficients obtained from molecular dynamics simulations. The line and shaded region represent the mean and standard deviation of 1,000 bootstrap samples, as described in **Section 2.4.** Left: Using unscaled diffusion coefficient values obtained from simulation. Right: Using diffusion coefficients scaled to the codeine-polyurea diffusion coefficient value used by Muro-Suñé, et al.

When computing the release profiles using the raw values computed from our simulations, we observed a significant amount of codeine and hexanal released into the water in picoseconds. While these release profiles might be unrealistic, we understand that this discrepancy from reality comes primarily from our simulation method to compute the diffusion coefficient. However, when we scale the diffusion coefficients to a value nearer to experiments, the release profiles become more realistic. While the trends seen in the diffusion and partition coefficients we computed from simulation qualitatively make sense based on our understanding of the chemistries involved, we are, unfortunately, unable to definitively claim that our method provides qualitative accuracy of the final computed release profiles, since we were unable to find any information of the release profile of hexanal in PU.

There is much room for improvement in the approach we have developed, which we describe in the conclusion (**Section 4**). That said, we have succeeded in developing a framework for a purely predictive model for the release profile of fragrance molecules from simulation data that can be expanded upon and improved in future iterations of this class.

4. Conclusion

In summary, we developed a multi-step method utilizing Martini simulations and a macroscale diffusion model used by Muro-Suñé and coworkers to predict the release profiles of codeine and hexanal, though the method can be extended to other small molecules. The predictive models of Muro-Suñé required experimental data to compute the partition and diffusion coefficients, but our simulation-based approach can provide these values purely computationally. These values, which qualitatively agree with our understanding of the relevant chemistries, are then used in the macroscale model to create a release profile. We compare our predicted release profiles to experimental data on a similar system studied by Muro-Suñé and coworkers.

We have established a foundation for the MD simulation, but much work can be done to improve the model created here, detailed in the following section. Through this project, we have gained a better understanding of a range of computational methods, allowing us to expand our professional development and interdisciplinary experience.

Possible Directions for Future Work

Extending this approach: Our approach could be further validated by computing release profiles for systems for which there is experimental data and qualitatively comparing the computed release profiles. We also developed this approach with the goal of making it flexible enough to be applied to mixtures of small numbers of fragrance molecules; some additional work is needed to realize this goal.

Partition simulations: One option is further validation of our approach include simulating with different box sizes and/or different length polyurea chains to validate that there are no finite size effects, simulating the

reverse path (starting with $\lambda = 0$ to $\lambda = 1$) to ensure thermodynamic path independence. Possible alternatives for the free energy calculations that could also provide validation or improvement include free energy perturbation, Bennett's acceptance ratio, or adjusting the TI parameters.

Diffusion simulations: It is generally infeasible to simulate diffusion through high-density, glassy polymers due to their long relaxation times. This is apparent in the order-of-magnitude difference between the diffusion coefficient in our melt-like simulations and the more realistic values predicted by Muro-Suñé and coworkers. One possible approach to bridge this gap is to use scaling relations (i.e., Casalini-Roland scaling) to develop the scaling relation between diffusion coefficient and polymer density, and use that relationship to extrapolate to more realistic conditions that cannot be well-simulated.

Improved simulation models: One could use atomistic simulations of the polyurea to obtain a more accurate coarse-grained model of the polyurea.

Macroscale model: One can attempt to use alternative macroscale models or vary capsule size parameters.

Alternate approaches: One could attempt to use theoretical approaches, rather than simulation, to compute partition or diffusion coefficients.

Code Availability

We include our code used to generate simulation data files (including our Avogadro-minimized molecular structure files for codeine and hexanal and nonbonded potential parameter tables), sample simulation scripts, simulation analysis scripts, our implementation of the release profile solver, and a further description of how to use and/or modify each script at https://github.com/NRT-hackathon/2023-IFF.

Acknowledgments

The authors express their gratitude to the project mentor, Dr. Shyam Vyas, for constant guidance and directions, and the course instructors, Prof. Arthi Jayaraman and Prof. Austin Brockmeier, for their support and suggestions. This work was supported in part through the use of DARWIN computing system: DARWIN – A Resource for Computational and Data-intensive Research at the University of Delaware and in the Delaware Region, Rudolf Eigenmann, Benjamin E. Bagozzi, Arthi Jayaraman, William Totten, and Cathy H. Wu, University of Delaware, 2021, URL: https://udspace.udel.edu/handle/19716/29071

References

(1) Günay, K. A.; Berthier, D. L.; Jerri, H. A.; Benczédi, D.; Klok, H.-A.; Herrmann, A. Selective Peptide-Mediated Enhanced Deposition of Polymer Fragrance Delivery Systems on Human Hair. *ACS Appl. Mater. Interfaces* **2017**, *9* (28), 24238-24249. DOI: 10.1021/acsami.7b06569 (acccessed 2023-02-23T14:58:05).
(2) Vethamuthu, M.; Lira, S.; Diantonio, E.; Fares, H. Review of innovations to improve fragrance bloom, release, and retention on skin from surfactant-rich cosmetics. *Journal of Cosmetic Science* **2017**, *68* (1), 133-136.
(3) Carvalho, I. T.; Estevinho, B. N.; Santos, L. Application of microencapsulated essential oils in cosmetic and personal healthcare products - a review. *International Journal of Cosmetic Science* **2016**, *38* (2), 109-119. DOI: 10.1111/ics.12232 (acccessed 2023-04-20T02:08:52).
(4) Martins, I. M.; Barreiro, M. F.; Coelho, M.; Rodrigues, A. E. Microencapsulation of essential oils with biodegradable polymeric carriers for cosmetic applications. *Chemical Engineering Journal* **2014**, *245*, 191-200. DOI: 10.1016/j.cej.2014.02.024 (acccessed 2023-04-18T17:39:40).
(5) Xiao, Z.; Sun, P.; Liu, H.; Zhao, Q.; Niu, Y.; Zhao, D. Stimulus responsive microcapsules and their aromatic applications. *Journal of Controlled Release* **2022**, *351*, 198-214.
(6) Trojer, M. A.; Nordstierna, L.; Bergek, J.; Blanck, H.; Holmberg, K.; Nydén, M. Use of microcapsules as controlled release devices for coatings. *Advances in colloid and interface science* **2015**, *222*, 18-43.
(7) Jyothi, S. S.; Seethadevi, A.; Prabha, K. S.; Muthuprasanna, P.; Pavitra, P. Microencapsulation: a review. *Int. J. Pharm. Biol. Sci* **2012**, *3* (2), 509-531.
(8) Rothstein, S. N.; Federspiel, W. J.; Little, S. R. A unified mathematical model for the prediction of controlled release from surface and bulk eroding polymer matrices. *Biomaterials* **2009**, *30* (8), 1657-1664. DOI: 10.1016/j.biomaterials.2008.12.002 (acccessed 2023-04-17T18:38:15).
(9) Muro-Suñé, N.; Gani, R.; Bell, G.; Shirley, I. Model-based computer-aided design for controlled release of pesticides. *Computers & chemical engineering* **2005**, *30* (1), 28-41.
(10) Muro-Suné, N.; Gani, R.; Bell, G.; Shirley, I. Predictive property models for use in design of controlled release of pesticides. *Fluid phase equilibria* **2005**, *228*, 127-133.
(11) Hossain, S.; Kabedev, A.; Parrow, A.; Bergström, C. A. S.; Larsson, P. Molecular simulation as a computational pharmaceutics tool to predict drug solubility, solubilization processes and partitioning. *European Journal of Pharmaceutics and Biopharmaceutics* **2019**, *137*, 46-55.
(12) Zhao, H.; Fei, X.; Cao, L.; Zhang, B.; Liu, X. The Fabrication of Fragrance Microcapsules and Their Sustained and Broken Release Behavior. *Materials (Basel)* **2019**, *12* (3), 393. DOI: 10.3390/ma12030393 (acccessed 2023-04-17T19:30:30).
(13) Bogdanic, G.; Fredenslund, A. Revision of the group-contribution Flory equation of state for phase equilibria calculations in mixtures with polymers. 1. Prediction of vapor-liquid equilibria for polymer solutions. *Industrial & engineering chemistry research* **1994**, *33* (5), 1331-1340.
(14) Zielinski, J. M.; Duda, J. L. Predicting polymer/solvent diffusion coefficients using free-volume theory. *AIChE Journal* **1992**, *38* (3), 405-415.
(15) Souza, P. C. T.; Alessandri, R.; Barnoud, J.; Thallmair, S.; Faustino, I.; Grünewald, F.; Patmanidis, I.; Abdizadeh, H.; Bruininks, B. M. H.; Wassenaar, T. A.; et al. Martini 3: a general purpose force field for coarse-grained molecular dynamics. *Nature Methods* **2021**, *18* (4), 382-388. DOI: 10.1038/s41592-021-01098-3 (acccessed 2023-03-09T20:59:46).
(16) Hanwell, M. D.; Curtis, D. E.; Lonie, D. C.; Vandermeersch, T.; Zurek, E.; Hutchison, G. R. Avogadro: an advanced semantic chemical editor, visualization, and analysis platform. *Journal of Cheminformatics* **2012**, *4* (1), 17. DOI: 10.1186/1758-2946-4-17 (acccessed 2023-04-25T10:18:53).
(17) Agrawal, V.; Holzworth, K.; Nantasetphong, W.; Amirkhizi, A. V.; Oswald, J.; Nemat-Nasser, S. Prediction of viscoelastic properties with coarse-grained molecular dynamics and experimental validation for a benchmark polyurea system. *Journal of Polymer Science Part B: Polymer Physics* **2016**, *54* (8), 797-810. DOI: 10.1002/polb.23976 (acccessed 2023-03-23T19:39:52).
(18) Marrink, S. J.; Risselada, H. J.; Yefimov, S.; Tieleman, D. P.; De Vries, A. H. The MARTINI Force Field: Coarse Grained Model for Biomolecular Simulations. *The Journal of Physical Chemistry B* **2007**, *111* (27), 7812-7824. DOI: 10.1021/jp071097f (acccessed 2023-03-07T20:51:56).
(19) Thompson, A. P.; Aktulga, H. M.; Berger, R.; Bolintineanu, D. S.; Brown, W. M.; Crozier, P. S.; in't Veld, P. J.; Kohlmeyer, A.; Moore, S. G.; Nguyen, T. D. LAMMPS-a flexible simulation tool for particle-based materials modeling at the atomic, meso, and continuum scales. *Computer Physics Communications* **2022**, *271*, 108171.

(20) Maginn, E. J.; Messerly, R. A.; Carlson, D. J.; Roe, D. R.; Elliot, J. R. Best Practices for Computing Transport Properties 1. Self-Diffusivity and Viscosity from Equilibrium Molecular Dynamics [Article v1.0]. *Living Journal of Computational Molecular Science* **2020**, *2* (1). DOI: 10.33011/livecoms.1.1.6324 (acccessed 2023-05-11T02:06:49).

Appendix

Section A1: Descriptions of Variables in Equations

Table A1: Nomenclature for Equation 1

$$\frac{dC_d}{dt} = \frac{-DA_i}{hV_i} K_{m/d}\, C_{d,init} \exp\left(\frac{-DA_i}{hV_r} K_{m/d}\left(\frac{K_{m/r}}{K_{m/d}} + \frac{V_r}{V_i}\right) t\right)$$

dC_d/dt	rate of change of concentration of FM inside the capsule
$C_{d,initial}$	initial concentration of FM inside capsule
V_r	volume of the release medium
V_i	internal volume of the microcapsule ($= \frac{4}{3}\pi R_i^3$, where R_i is the radius of the microcapsule size)
A_i	outer surface area of microcapsule ($= 4\pi R_i^2$)
h	microcapsule wall thickness
D	diffusion coefficient of FM through polymer wall
$K_{m/d}$	partition coefficient of FM between polymer and environment inside the capsule
$K_{m/r}$	partition coefficient of FM between polymer and environment outside the capsule

Table A2: Nomenclature for Equation 2

$$\Delta G = \int_0^1 \langle \frac{\partial U}{\partial \lambda} \rangle_\lambda \, d\lambda \approx \int_0^1 \frac{\langle U(\lambda + d\lambda) - U(\lambda) \rangle_\lambda}{d\lambda} d\lambda$$

ΔG	change in Gibbs free energy associated with removing the FM from its environment (kJ/mol)
U	total energy of the simulation (kJ/mol)
λ	coupling parameter

Table A3: Nomenclature for Equation 3

$$D = \frac{1}{6} \lim_{t \to \infty} \frac{d}{dt} \langle \frac{1}{N} \sum_{i=1}^{N} |r_i(t) - r_i(0)|^2 \rangle$$

D	diffusion coefficient of FM through polyurea wall (m^2/s)
t	time (s)
N	number of molecules diffusing
r_i	initial position of the center of mass of all diffusing molecules (m)

Table A4: Nomenclature for Equation 4

$$C_d(t) = \frac{V_r\, C_{d,init}}{V_i\left(\frac{K_{m/r}}{K_{m/d}} + \frac{V_r}{V_i}\right)} \left[\exp\left(\frac{-DA_i}{hV_r} K_{m/d}\left(\frac{K_{m/r}}{K_{m/d}} + \frac{V_r}{V_i}\right) t\right) - 1\right] + C_{d,init}$$

C_d(t)	concentration of the FM as a function of time (g/m^3)
$C_{d,init}$	initial concentration of FM
V_i	initial capsule volume
V_r	release medium volume
$K_{m/r}$	partition coefficient of the FM between capsule wall and release medium
$K_{m/d}$	partition coefficient of the FM between capsule wall and capsule medium
D	diffusion coefficient of the FM through capsule wall (m^2/s)
A_i	initial outer surface area of capsule (m^2)
h	thickness of the capsule wall (m)

Section A2: Description of Martini 3 Beads

Bead assignment is a crucial step in building accurate molecular models and can be created manually or through the use of artificial intelligence and machine learning topology methods. In our study, we utilized a combination of the Martini bead library and to group atoms together into appropriate bead types for modeling water, polyurea, hexanal, and codeine. A hydrogen donor/acceptor or charged label was added to the bead if necessary for the chemistry of that molecule. The numbers following the bead type indicate the attraction level of the bead, with smaller numbers indicating higher attraction. These bead types result in the assignment of numbers from the Martini 3 interaction block, which then translates to corresponding sizes and interaction levels of various organic blocks.[14]

Compared to previous versions of the Martini force field, Martini 3 can accurately represent aromatic structures and allows for interactions between different bead sizes. This is particularly important when modeling codeine, which contains a phenanthrene ring system and requires different-sized beads in its model.

Table A5: Martini Bead Label Descriptions

Bead Type	**P**	Polar
	N	Intermediate/Non-polar
	C	Apolar
Interaction Level	**0-1**	Hyper Attractive
	2-3	Super Attractive
	4-5	Attractive
	6	Almost Attractive
Bead Size	**none**	Regular (σ = 0.47 nm)
	S	Small (σ = 0.41 nm)
	T	Tiny (σ = 0.34 nm)
Bead Labels	**a**	Hydrogen Donor
	d	Hydrogen Acceptor
	q	Partial charge

Section A3: Supplemental Results

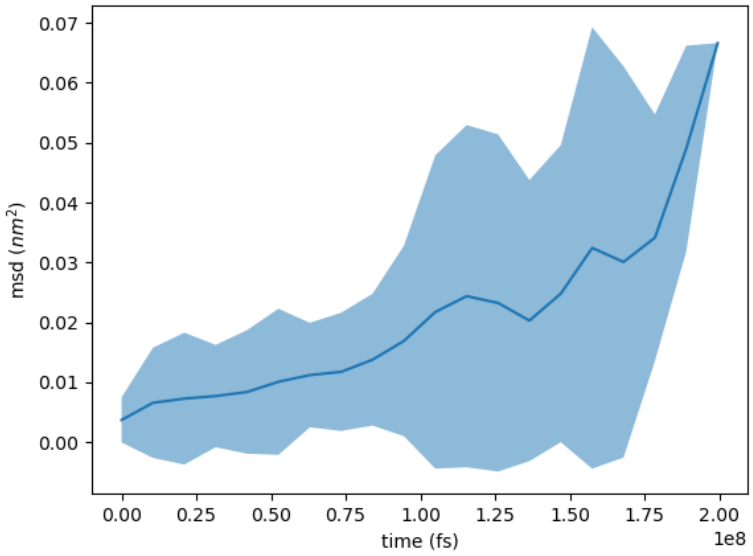

Figure A1: Example MSD data for codeine in polyurea for a diffusion simulation, simulated with polyurea-polyurea interactions modeled using the LJ potential with prescribed Martini parameters and polyurea density matching that of the bulk experimental density of polyurea. Two aspects of this data would be concerning if used for calculation of the diffusion coefficient. First, the codeine molecule does not displace a significant distance (the box size here is 10nm, so the MSD is <1% of the box size), so we would have poor sampling and an unreliable diffusion coefficient. Second the data is not particularly linear over the course of the simulation, indicating that even longer simulations would be required to compute the diffusion coefficient reliably. Both of these considerations are somewhat expected for glassy systems, where the relaxation time can be much longer than obtainable in molecular simulations.

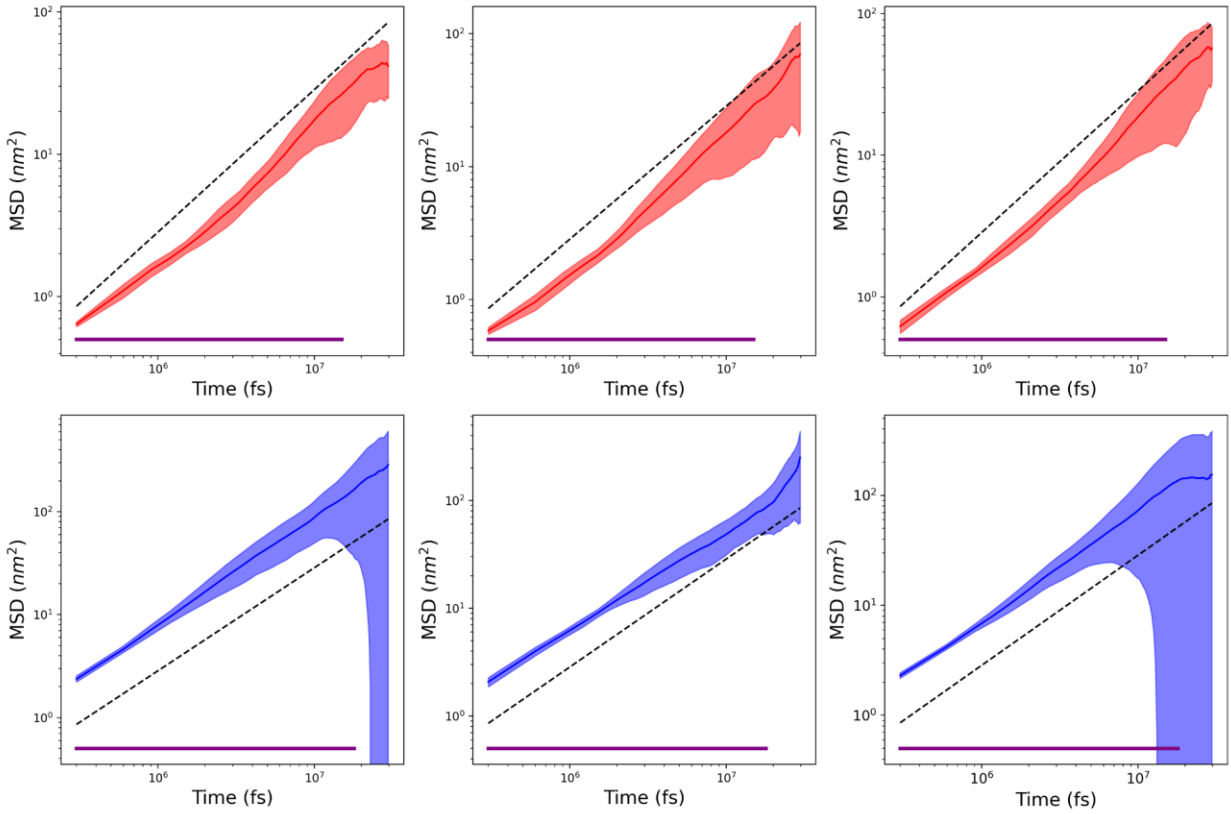

Figure A2: Log-log plots of the MSD of the diffusing molecules vs simulation time in the Diffusion simulations. Colored lines and shaded regions represent the mean and standard deviation of the 5 diffusing molecules in each simulation. The red plots (top row) denote codeine simulations and the blue plots (bottom row) denote hexanal simulations, and the three plots across each row show the data from 3 independent simulation trials. The dotted black line is a reference line with slope 1. The MSD vs time plot should have a slope approximately 1 in the diffusive regime used to calculate the diffusion coefficient. The purple line at the top of each plot indicates the range of data over which the diffusion coefficient was calculated. While the data over these ranges may not perfectly follow a slope of 1, it is close. It is expected that simulating a greater number of diffusing molecules would result in a slope nearer to 1.

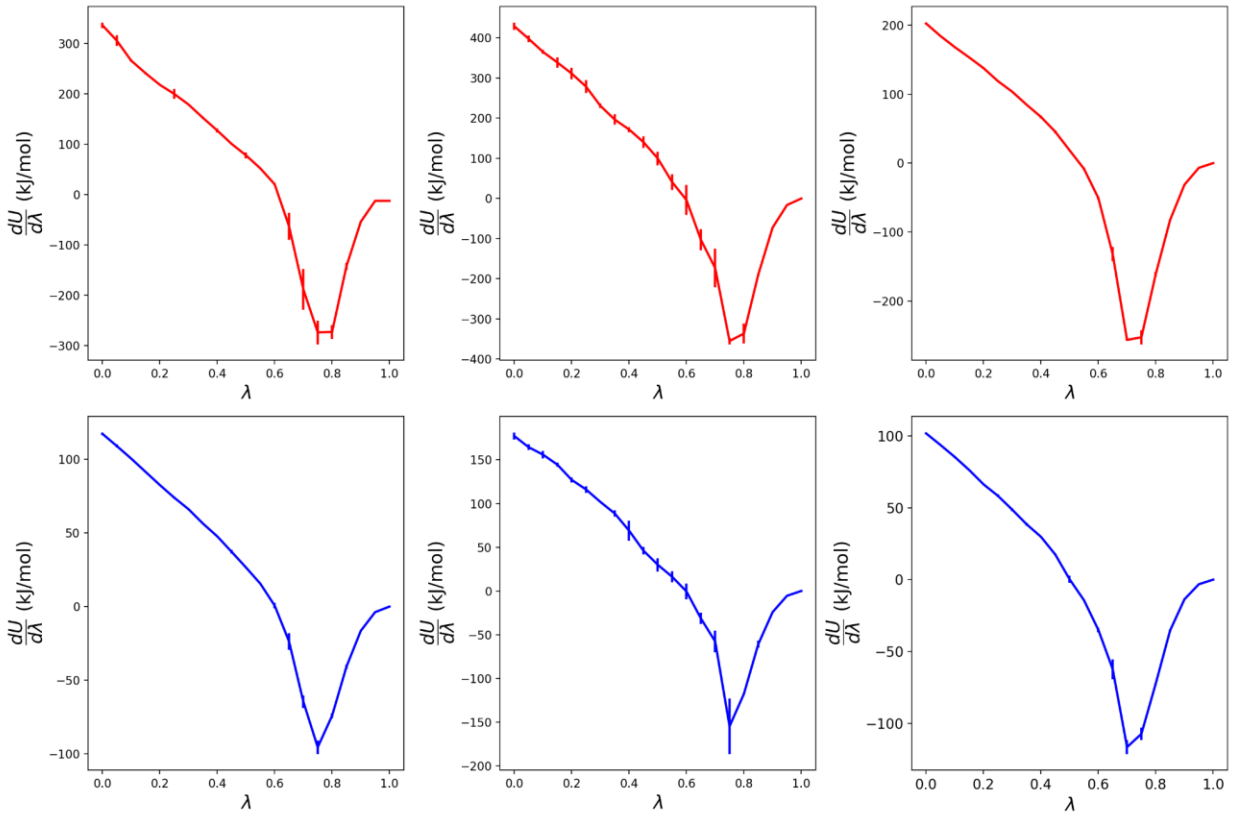

Figure A3: Plots of dU/dλ vs λ obtained from partition coefficient simulations. Red plots are for codeine and blue plots are for hexanal. The left, center, and right plots are data for the simulations in environments of pure FM, polyurea, and water, respectively. The error bars represent the standard deviation of three independent trials. This data was integrated using the trapezoid method to obtain the changes in free energy presented in **Table 2.**

Section A4: Specifics of Computing Partition Coefficients Using Thermodynamic Integration

In our simulations, λ is 1 when there is full interaction between the FM and its surrounding molecules, and λ is 0 when there are no interactions. This is implemented using a soft LJ potential (**Eq. A1**), where n = 2 and α = 0.5 are values commonly used in such simulations. All ε and σ are defined according to the Martini model and mapping described in **Section 2.1**. It can be seen from **Eq.4** that for λ = 1, the potential reduces to the standard LJ potential, while at λ = 0, the energy is 0.

For our simulations, we follow the schedule shown in **Figure 3**, where we run the simulation at each value of λ for 100,000 timesteps, including a 92,000 equilibration stage and an 8,000 timestep production stage, over which the ensemble average of the energy change (numerator of the integrand in the right-most expression of **Eq. 3**) is computed by averaging values collected every 20 timesteps. The energy change is computed using the forward finite difference using a step in the coupling parameter dλ = 0.002, and the energy derivative is calculated at λ values decreasing from 1 to 0 in steps of Δλ = 0.05. The exception to this is at λ = 0: Here, we cannot compute the forward difference derivative since that would result in computing energies at the unphysical λ = -0.002. Instead, we compute the backward difference derivative, simulating at λ = dλ = 0.002 and computing the energy difference between λ = 0.002 and λ = 0. Once the energy derivatives are calculated at all λ. The integral in **Eq. 2** is approximated using the trapezoid method.

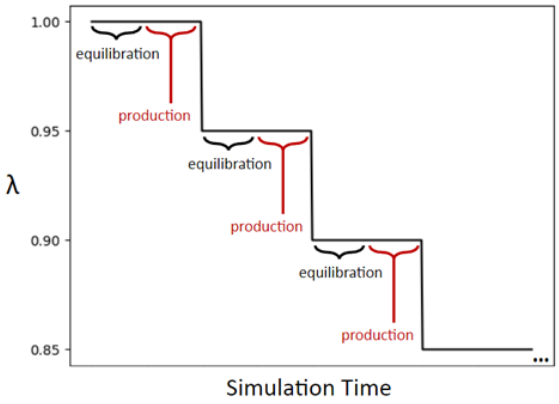

Figure A4. Schematic describing progression of the coupling parameter (λ) over the course of the partition coefficient simulations

$$U(r) = \lambda^n * 4\epsilon \left\{ \frac{1}{\left[\alpha(1-\lambda)^2 + \left(\frac{r}{\sigma}\right)^6\right]^2} - \frac{1}{\alpha(1-\lambda)^2 + \left(\frac{r}{\sigma}\right)^6} \right\} \qquad \text{Eq. A1}$$

To compute the partition coefficients of the FM between the capsule wall and the inside of the capsule ($K_{m/d}$) and between the capsule wall and the release medium ($K_{m/r}$). We need to compute the free energy changes associated with removing the FM from each environment (pure FM inside the capsule, polyurea in the capsule wall, and water outside the capsule) using **Eq. 2**, denoted $\Delta G_{s->0}$, where s is the environment by which the FM is surrounded.

We can compute the free energy change between two environments, s1 and s2, using the equation:

$$\Delta G_{s1\to s2} = \Delta G_{s1\to 0} - \Delta G_{s2\to 0}$$

and final compute the partition coefficient using the relationship:

$$\log\left(K_{s1/s2}\right) = \frac{\Delta G_{s1\to s2}}{2.303RT}$$

Section A5: Simulation Snapshots:

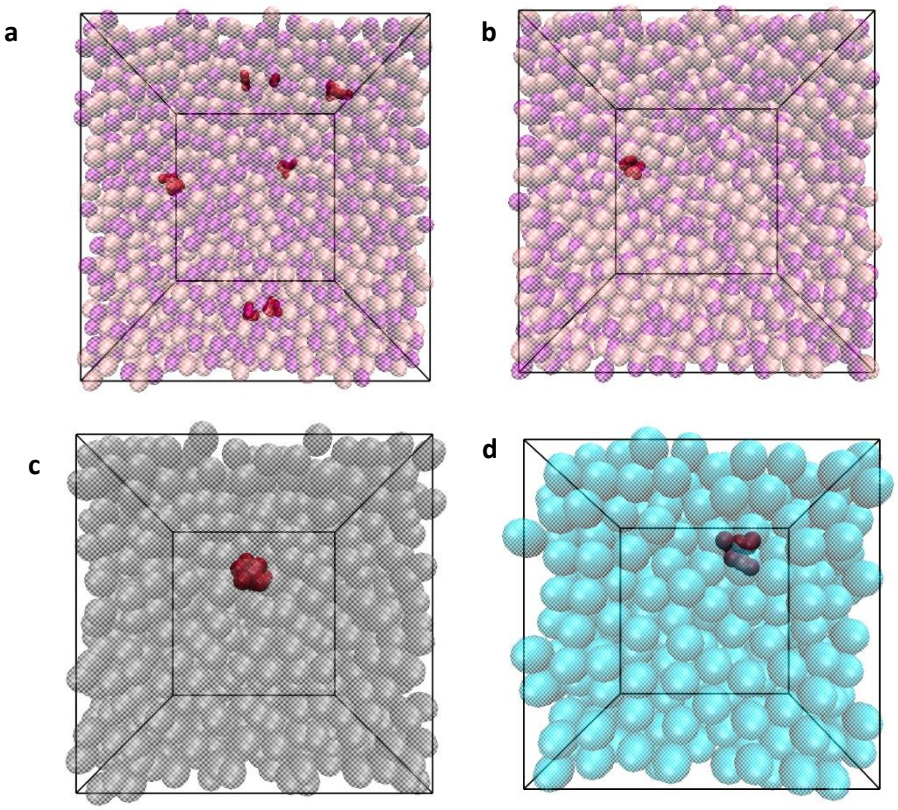

Figure A5: Simulation snapshots from our simulations. (a) diffusion simulation of codeine (red) in polyurea (pink and purple transparent), (b) partition coefficient simulation of codeine (red) in polyurea(pink and purple transparent), (c) partition coefficient simulation of codeine (red) in codeine (gray transparent), (d) partition coefficient simulation of codeine (red) in water (blue transparent)

Section A6: Parameters for the ODEs (Eqs. 1 and 4)

Table A6: Additional parameters used in Eq. 4 to solve for the total release profile shown in Fig. 4

Parameters Describing Microcapsule Size	h (nm)	Mean radius (nm)	Radius Standard Deviation (nm)	Radius Range Considered (nm)	Radius step (nm)
	2.86	129	30	29 - 329	10
Additional Parameters Used for Solving Eq. 4	V_r (cm^3)	V_d (cm^3)	$C_{d,\ init}$ (kg/m^3)		
	400	0.485	Bulk Density of FM (1.2 for codeine, 0.814 for hexanal)		